32nd Congress of the International Council of the Aeronautical Sciences
September 6-10, 2021
Pudong Shangri-La, Shanghai, China

A NUMEIRCAL PREDICTION OF THE AIRCRAFT ICING METEOROLOGICAL ENVIRONMENT

Qilei.Guo[1,2], Weimin.Sang[1,*], Junjie.Niu[1] & Aoxiang.Qiu[1]

[1]School of Aeronautics, Northwestern Polytechnical University, Xi'an 710072, China;
[2] School of Aeronautics Engineering, Civil Aviation Flight University of China, Guanghan 618307, China

Abstract

Aircraft icing is the essential menace to flight safety. An accurate prediction of the aircraft icing meteorological environment, combining geographical features is a critical ingredient to the aircraft de-/anti- icing. In this paper, a numerical method to accurately predict icing meteorological parameters is established. The Weather Research and Forecasting (WRF) is applied and four microphysics schemes are evaluated to determine the optimal parameterization scheme. The results show that the Purdue Lin microphysics schemes yields superior performance in predicting both evolution tendency and numerical precision. The BP neural network based on the deviation of the observed and predicted icing parameters is established. The icing meteorological parameters corrected by the constructed BP neural network are better consistence with observed values than values directly predicted by the WRF with the Purdue Lin scheme. The paper is the preliminary work of aircraft icing rapid prediction and aims to provide precise input data for follow-up aircraft icing numerical prediction.

Keywords: numerical prediction, optimization, icing situation field, WRF, BP neural network

1. Introduction

Aircraft icing is the essential menace to flight safety [1]. When the aircraft is exposed in high-altitude clouds, the supercooled liquid droplets impact the aircraft surface and induce heat and mass transfer, further resulting in icing accretion on the windward surface of the aircraft, such as the airfoils, engine inlet, sensors, etc., which perhaps causes severe aerodynamic and flight mechanical effects and thus threatens aircraft flight safety [2]. The National Transportation Safety Board (NTSB) once announced that the natural icing problem is one of the "Most Wanted Aviation Transportation Safety Improvements" [3]. According to the statistics of the Federal Aviation Administration (FAA), there were 388 flight accidents caused by icing during the decade from 1990 to 2000. With the increase in flight density, there were 380 icing-related accidents during the five years from 2003 to 2008. There also have been many severe flight accidents recently caused by ice accretion in China, for example, the Anhui air crash in 2006 caused 40 deaths. Therefore, it is of urgent practical significance to systematically carry out researches on the flight safety of aircraft during icing encounters.

The intensity of aircraft icing and the hazards to flight safety mainly depend on the icing meteorological conditions, such as liquid water content (LWC), water droplet median volume diameter (MVD), relative humidity (RH), cloud temperature pressure and cloud range. The measurement results of icing meteorological conditions in North America have laid the foundation of FAR Appendix C and Appendix O. Appendix C and appendix O specifies atmospheric icing conditions and supercooled large droplets (SLD) icing conditions respectively. In appendix C, the maximum continuous or intermittent intensity of atmospheric icing conditions are both defined by the variables of the cloud LWC, MVD, the ambient cloud temperature and the interrelationship of these three variables. In appendix O, SLD icing conditions are defined by the parameters of altitude, vertical and horizontal extent, temperature, liquid water content, and water mass distribution as a function of drop diameter distribution [4].

Many researchers have obtained a variety of achievements on numerically predicting icing meteorological conditions. Nygaard et al. [5] concluded that the spatial resolution (with grid spacing of 0.333 km) used in NWP (Numerical Weather Prediction) models is a decisive factor in the correct prediction of icing at ground level. Davis et al. [6] evaluated nine WRF physics parameterization combinations for icing episodes at a wind park in Sweden. Sergio Fernández-González et al. [7] indicated moisture, wind direction, temperature, atmospheric stability, and wind shear were decisive in the appearance of icing by analyzing a real severe icing case using WRF. Merino et al. [8] used four microphysics and two planetary boundary layer schemes, to investigate the capability of the WRF model to detect regions containing supercooled cloud drops. Faisal et al. [9] investigated weather conditions related to aircraft icing to improve ice prediction. Mei et al. [10] studied the application of the High-Resolution Rapid Refresh model in ice accretion prediction and improved it. Bowyer et al. [11] used satellite data to infer the icing potential in Europe, Asia, and Australia and compared it with the measured results. Wang et al. [12] proposed the icing index algorithm is calculated using linear interpolation and based on temperature and relative humidity (RH) curves obtained from radiosonde observations in China.

The cloud and fog parameter envelopes that are consistent with Chinese icing meteorological characteristics are of great significance to the airworthiness certification of the domestic large aircraft. Therefore, it is urgent to confirm applicative icing weather conditions, in order to provide strong support for the airworthiness certification of the domestic large aircraft. Survey results have shown that aircraft icing accidents usually occur in coastal, plateau, and water-rich regions. Chengdu Shuangliu International Airport (CTU) is located in the southwestern region of China, which is climatically characterized by abundant rainfall, high humidity and less sunshine [13]. Civil transports are prone to be interfered by fog in winter during the approach and climb stages in such weather condition. According to the statistics, in recent five years from 2014 to 2018, there are total of 35 low visibility weather occurred during the approach and climb stages in CTU, with an annual average of 7 times, mainly from October to January of the following year. The icing meteorological environment, combining geographical features has become one of the important factors restricting aircraft flight performance and threatening aviation safety.

The aim of present work is to establish a numerical model for accurate prediction of aircraft icing situation field near the ground by using the Weather Research and Forecasting (WRF), to provide precise input data for follow-up aircraft icing numerical test. Firstly, the two-level nested mesh technology considering geographical features, is employed. Further, the multiple combinations of microphysics schemes are evaluated, and the optimal physical process parameterized combination for the aircraft ice accretion is determined. On this basis, the pressure and temperature fields are obtained. Finally, based on the various predicted and measured meteorological values, BP neural network is employed to correct the future icing meteorological conditions forecasting by the WRF pattern. The paper is the preliminary work of aircraft icing rapid prediction and aims to provide precise input data for follow-up aircraft icing numerical prediction.

2. Numerical Configuration

The work of this paper is divided into two parts: one part is to determine the optimal physical process parameterized combination based on the WRF model and output the predicted icing meteorological parameters; the other part is to construct a BP neural network for the deviation between the predicted and observed values of the icing meteorological parameter, and to calculate the future predicted value. The schematic diagram of aircraft icing situation field prediction is shown in Figure 1.

2.1 WRF Model Setup

The mesoscale numerical weather prediction model used in this study is the Advanced Research WRF (ARW) modeling system, version 4.1.2. In order to verify with the observed values from meteorological observatory, the numerical simulation take the geographic location of Chengdu Shuangliu Meteorological Observation Station (103.55°E, 30.35°N) as the center point of the simulated area, from 2021-04-10 00:00:00 UTC to 2021-04-16 00:00:00 UTC. Initial and boundary conditions were retrieved from National Centers for Environmental Prediction (NCEP) Global Forecast System analyses, with 1° horizontal grid spacing and a temporal resolution of 6 h. In order to save computation cost, simulations are carried out by applying two levels of nesting, which means that the inner model domain with the finer resolution is embedded into the outer model domain with the coarser resolution, following a one-way nesting strategy, as shown in Figure 2. Horizontal resolution of the domains was 5 and 1 km, respectively, and vertical resolution was set to 34 sigma linear levels.

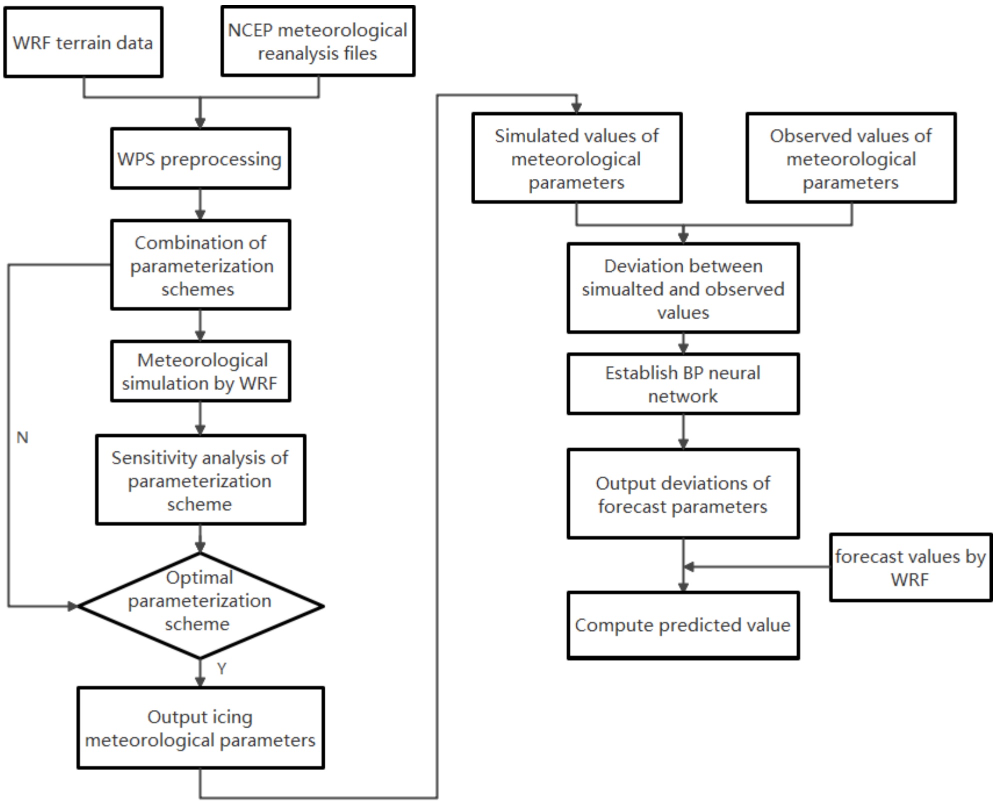

Figure 1 – The schematic diagram of aircraft icing situation field prediction.

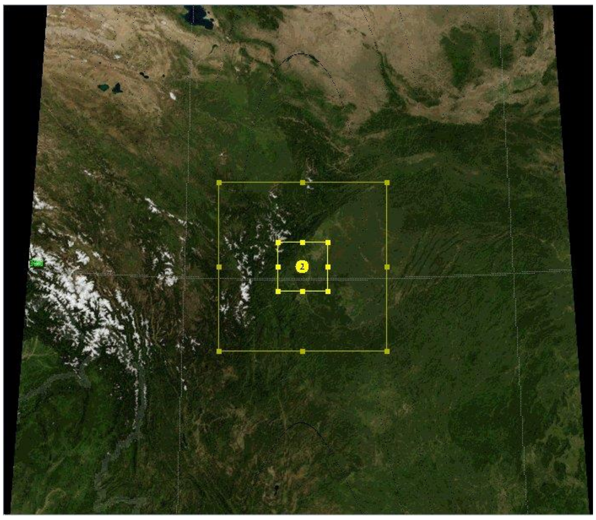

Figure 2 – The nested domain of numerical simulation.

The selected parameterization schemes were as follows: Dudhia scheme [14] and the Rapid Radiative Transfer Model [15] for shortwave radiation and longwave radiation respectively, and Yonsei University scheme [16] for Planetary Boundary layer. MM5 similarity surface layer scheme described by Fairall [17], and Noah Land Surface Model [18], which is a four-layer soil temperature and moisture model with canopy moisture and snow cover estimation, are considered. The Kain-Fritsch cumulus scheme [19] is employed to both nested domains.

In order to optimize the parameterization schemes, four microphysics schemes were tested: the Purdue Lin microphysics scheme, WRF single-moment six-class scheme, Thompson six-class microphysics scheme and Morrison six-class double-moment scheme. Purdue Lin microphysics scheme [20], a one-dimensional cloud model, takes in consideration the effects of entrainment, cloud microphysics, pressure perturbation, lateral eddy diffusion, and vertical eddy diffusion. WRF single-moment six-class (WSM6) scheme [21] predicts the rainfall amount becoming larger but rain distribution becoming narrower as the number of classification of hydrometeors is increasing. And WSM6 is capable of improving the simulated precipitation by shifting it southward toward the observation. Thompson six-class microphysics scheme [22] incorporates prognostic equations for the mass concentration of five hydrometeors: cloud water, cloud ice, rain, snow, and graupel, and has a great performance in the prediction of LWC, as special attention is paid to the formulation of the snow category. The Morrison six-class double-moment scheme [23], based on the full two-moment scheme, predicts the mass concentration of five hydrometeors (in consistence with the Thompson scheme), in addition to the number concentration of four species: cloud ice, snow, rain, and graupel. The prediction of both mass mixing ratio and number concentration of four water species allows a more robust description of size distributions.

Three indicators which are employed to evaluate above four microphysics schemes in this work, are: (1) mean absolute error, MAE; (2) root mean absolute error, RMAE; (3) Pearson correlation coefficient, *r*. The detailed indicator expressions are demonstrated as follows

$$\mathrm{MAE} = \frac{1}{N}\sum\left|y^{meas} - y^{pred}\right| \tag{1}$$

$$\mathrm{RMAE} = \frac{1}{N}\sum\left|\left(y^{meas} - y^{pred}\right)/y^{meas}\right| \tag{2}$$

$$r = \frac{\sum\left(y^{meas} - \bar{y}^{meas}\right)\left(y^{pred} - \bar{y}^{pred}\right)}{\sqrt{\sum\left(y^{meas} - \bar{y}^{meas}\right)^2 \sum\left(y^{pred} - \bar{y}^{pred}\right)^2}} \tag{3}$$

Here, y^{meas} and y^{pred} are the observed and predicted values of icing meteorology parameters, $\bar{y}^{meas}$ and $\bar{y}^{pred}$ are the observed and predicted average values of icing meteorology parameters, N is the samples quantity.

2.2 Neural Network Design

The BP (Back Propagation) neural network used in this article is a multi-layer feedforward neural network with error back propagation. Because of its wide applicability and easy operation, it is currently the most widely used neural network model. The schematic diagram of the BP neural network is shown in Figure 3. The structure mainly includes input layer, hidden layer and output layer. The hidden layer contains one or more layers of neurons. It is learned through inverse retraining and the gradient descent algorithm is used. Finally, a non-linear mapping logic between input and output is established to minimize the network error. However, BP neural network also has disadvantages such as low learning efficiency, requires a large number of sample training, and falling into local optimal misunderstandings. At the same time, the determination of the number of network layers and neurons in BP neural network lacks theoretical methods and requires manual judgment.

In this work, the number of hidden layers of BP neural network is determined to be 2, and the number of hidden layer neurons is 16, so the constructed BP neural network has a 2-16-16-2 structure. Then the final determination is that the learning rate is 0.01, and the iteration error is 1e-6.

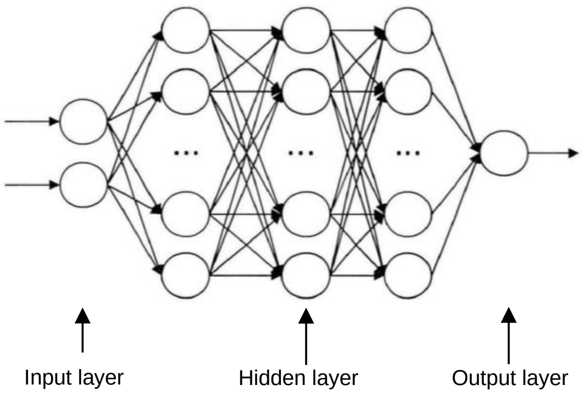

Figure 3 – The BP neural network structure diagram.

3. Validation and Results

The icing meteorological environment in the targeted domain is simulated by means of four microphysics schemes, and the optimal parameterization scheme is determined through error analysis among four schemes. The pressure and temperature comparison of the observed and predicted values at the domain's center point are demonstrated in Figure 4. In the set of figures, black line for observed values, red line for Morrison scheme, olive line for Thompson scheme, magenta line for WSM6 scheme and blue line for Purdue Lin scheme, respectively. As shown in the pressure comparison in Figure 4, all four parameterization schemes are capability of predicting the

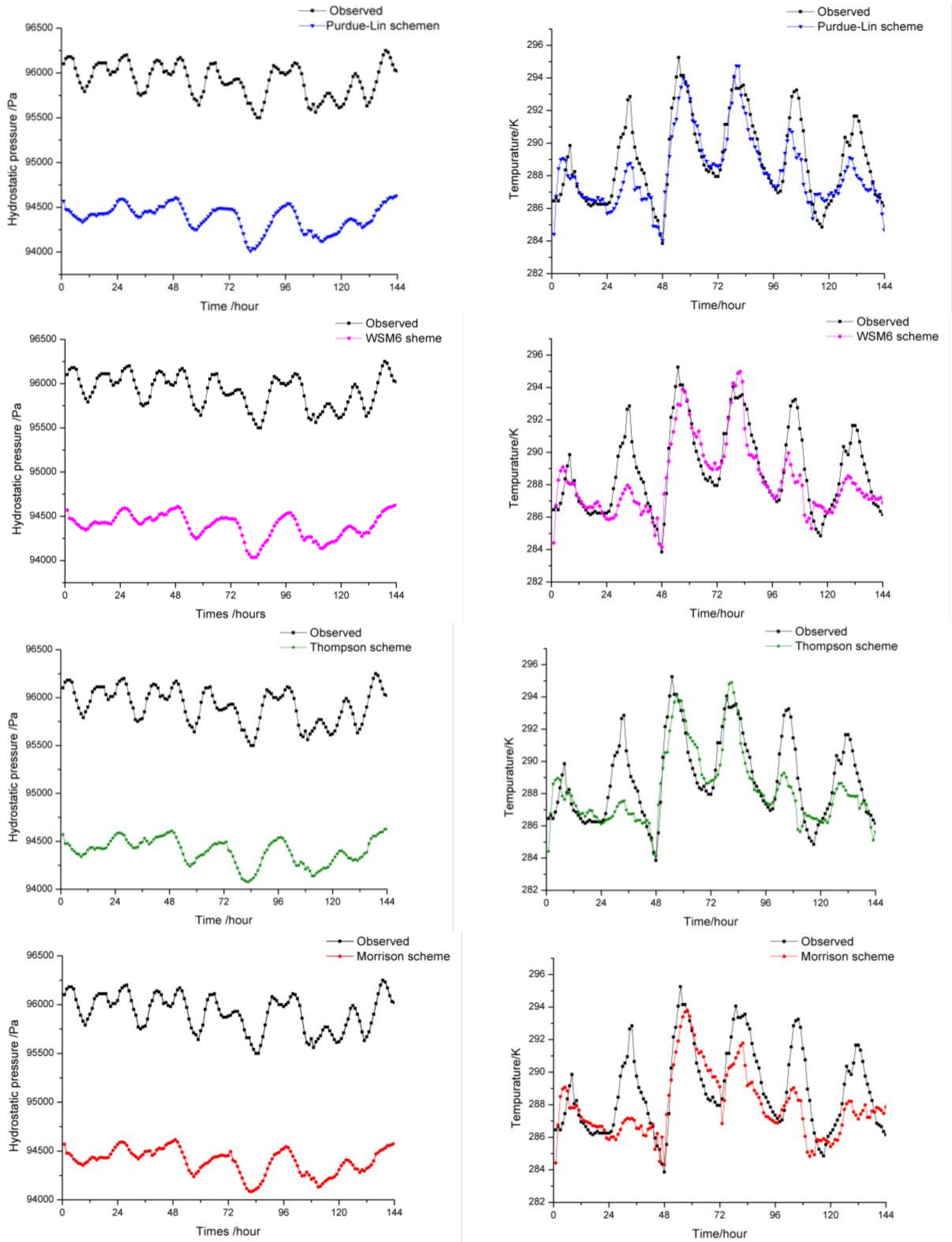

Figure 4 – The pressure (left) and temperature (right) comparison of observed and predicted values. (black line for observed values, red line for Morrison scheme, olive line for Thompson scheme, magenta line for WSM6 scheme and blue line for Purdue Lin scheme, respectively.)

pressure trend accurately. However, it is worth to note that the MAE and RMSE between the observed and simulated pressure are approximate to 1521.61~1531.02 Pa and 1.586%~1.596% as shown in Table 1. Relative to pressure simulation, all four parameterization schemes have more accurate performance in simulating temperature. Apart from the fact that there are three distinct deviations between the observed and simulated temperature (approximately at the 34^{h}, 106th, 132th time nodes), the predicted temperature values are consistent with observed values in both temporal evolution and numerical precision.

Error analysis of four microphysics schemes is illustrated in table 1. It is considered that two sets of variables are statistically strong correlation if Pearson correlation coefficient, *r,* between these two sets of variables is greater or equal to 0.6, and are extremely strong correlation if *r* is greater or equal to 0.8 correspondingly. Despite of distinct deviations of MAE and RMAE between the observed and simulated pressure, as shown in Table1, the Pearson correlation coefficients of microphysics schemes are approximate to 0.8, and Purdue Lin scheme has the best performance, the *r* indicator reaching up to 0.806. In the aspect of predicting temperature, Purdue Lin scheme still performs most accurately (MAE=1.12 and RMAE=0.388%). At the same time, the *r* indicator of Purdue Lin scheme reaches up to 0.845. Therefore, Purdue Lin scheme is determined to the optimal parameterization scheme and icing meteorological parameters predicted by Purdue Lin scheme are corrected by the following BP neural network.

Table 1 Error Analysis of four microphysics schemes prediction

	Pressure			Temperature		
	MAE	RMAE	*r*	MAE	RMAE	*r*
Morrison	1523.96	1.588%	0.798	1.64	0.566%	0.704
Thompson	1521.61	1.586%	0.789	1.32	0.454%	0.779
WSM6	1523.53	1.588%	0.795	1.26	0.432%	0.794
Purdue Lin	1531.02	1.596%	0.806	1.12	0.388%	0.845

The whole 144 hours data from 2021-04-10 00:00:00 UTC to 2021-04-16 00:00:00 UTC are divided into two parts: the first 140 hours data are used to training and validating the BP neural network, the rest 24 hours data is employed to test future data predicted by the constructed neural network. As shown in Figure 4, the corrected icing meteorological values are better consistence with observed values than values directly predicted by WRF with the Purdue Lin scheme.

The error analysis of Purdue Lin scheme prediction and BPNN correction is demonstrated in Table 2. The MAE and RMAE of pressure are decreasing from 1495.14 and 1.56% to 85.65 and 0.09% respectively. Correspondingly, the MAE and RMAE of temperature are decreasing from 1.41 and 0.49% to 0.70 and 0.24%. the *r* indicators of observed and BPNN corrected values are reach up to 0.831 and 0.900, which mean statistically strong correlation between these two sets of values.

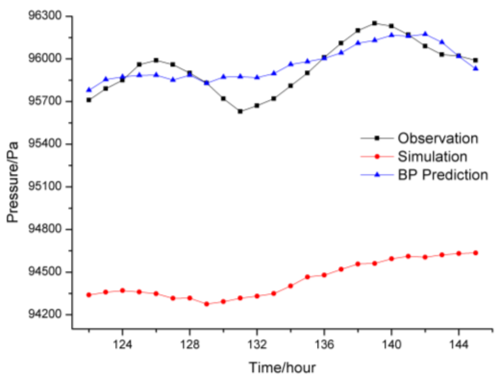

(a) pressure

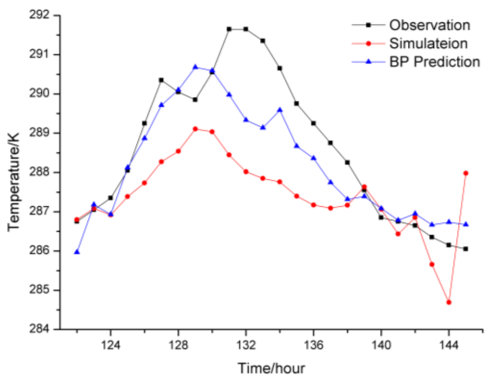

(b) temperature

Figure 5 – The comparison of Purdue Lin scheme prediction and BPNN correction

Table 2 Error Analysis of Purdue Lin scheme prediction and BPNN correction

	Pressure			Temperature		
	MAE	RMAE	*r*	MAE	RMAE	*r*
Purdue Lin	1495.14	1.56%	0.775	1.41	0.49%	0.709
BPNN corrected	85.65	0.09%	0.831	0.70	0.24%	0.900

4. Conclusions

An accurate prediction of icing meteorological environment, combining geographical features is a critical ingredient to the prediction of aircraft icing. In this paper, a numerical method to accurately predict icing meteorological parameters is established, by using the WRF pattern. Four microphysics schemes are evaluated to determine the optimal parameterization scheme. The results show that the Purdue Lin parameterization yielded superior performance in predicting both evolution tendency and numerical precision. Despite of distinct deviations of MAE and RMAE between the observed and simulated pressure, the Pearson correlation coefficients of pressure and temperature by Purdue Lin scheme reaches up to 0.806 and 0.845, which mean statistically strong correlation. The BP neural network based on the deviation of observed and predicted icing parameters is established. The icing meteorological parameters corrected by the constructed BP neural network are better consistence with observed values than values directly predicted by WRF with the Purdue Lin scheme. The MAEs of corrected pressure and temperature are dramatically decreasing. The statistical correlations between the observed and corrected values of icing meteorological parameters get further strengthened. This paper is the preliminary work of aircraft icing rapid prediction and aims to provide precise input data for follow-up aircraft icing numerical prediction.

5. Acknowledgement

This work has benefited greatly from the support of the National Key Project of China under grant GJXM92579 and the Open Fund of Key Laboratory of Icing and Anti/De-icing of China under grant IADL20200101.

6. Contact Author Email Address

Qilei Guo, email: cafuc_guoql@outlook.com

7. Copyright Statement

References

[1] Bragg M B. Rime ice accretion and its effect on airfoil performance. The Ohio State University, 1981.

[2] Cao Y H, Huang J S and Yin J. Numerical simulation of three-dimensional ice accretion on an aircraft wing. *International Journal of Heat and Mass Transfer*, Vol. 92, pp24-54, 2016.

[3] Ratvasky T P, Barnhart B P, Lee S. Current Methods Modeling and Simulating Icing Effects on Aircraft Performance, Stability, Control. *Journal of Aircraft*, Vol. 47, No. 1, pp. 201-211, 2010.

[4] Federal Aviation Administration. Part 25-Airworthiness Standards: Transport Category Airplanes. Available online: https://www.faa.gov/aircraft/air_cert/airworthiness_certification/std_awcert/std_awcert_regs/regs/

[5] Nygaard, B E K, Kristjánsson, J E, Makkonen L. Prediction of In-Cloud Icing Conditions at Ground Level Using the WRF Model. *Journal of Applied Meteorology and Climatology*, Vol. 50, No. 12, pp 2445-2459, 2011.

[6] Davis N, Hahmann A N, Clausen N E, Žagar M. Forecast of icing events at a wind farm in Sweden. *Journal of Applied Meteorology and Climatology*, Vol. 53, No. 2, pp 262–281, 2014.

[7] Sergio Fernández-González, José Luis Sánchez, Estíbaliz Gascón, Laura López, Eduardo García-Ortega, Andrés Merino. Weather Features Associated with Aircraft Icing Conditions: A Case Study. *The Scientific World Journal*, Vol. 2014, pp 279063, 2014.

[8] Merino, A, García‐Ortega, E, Fernández-González, S, Díaz‐Fernández J, Quitián‐Hernández L, Martín M L. Aircraft Icing: In‐Cloud Measurements and Sensitivity to Physical Parameterizations. *Geophysical Research Letters,* Vol. 46, pp 11559-11567, 2019.

[9] Boudala, F, Isaac G A, Wu D. Aircraft Icing Study Using Integrated Observations and Model Data. *Weather Forecast*, Vol. 34, pp 485–506, 2019.

[10] Xu, M, Thompson G, Adriaansen D R, Landolt S D. On the Value of Time-Lag-Ensemble Averaging to Improve Numerical Model Predictions of Aircraft Icing Conditions. *Weather Forecast*, Vol. 34, pp 507–519, 2019.

[11] Bowyer R L, Gill P G. Objective verification of global in-flight icing forecasts using satellite observations: Verification of WAFS icing forecasts using satellite observations. *Meteorological Applications*, Vol. 26, pp 610–619, 2019.

[12] Wang J H, Xie B Z, Cai J H. The Distribution of Aircraft Icing Accretion in China - Preliminary Study. *Atmosphere*, Vol. 11, No. 8, pp 876, 2020.

[13] Zhang x. Analysis on flight safety of Chengdu Shuangliu Airport under extreme weather condition. *Journal of Shenyang Aerospace University*, Vol. 35, No. 3, pp 81-86, 2018.

[14] Dudhia J. Numerical study of convection observed during the winter monsoon experiment using a mesoscale two‐dimensional model. *Journal of the Atmospheric Sciences*, Vol. 46, No. 20, 3077–3107, 1989.

[15] Mlawer E, Taubman S, Brown P, Iacono M, Clough S. Radiative transfer for inhomogeneous atmospheres: RRTM, a validated correlated‐k model for the longwave. *Journal of Geophysical Research*, Vol. 102, No. 14, pp 16,663–16,682, 1997.

[16] Hong S Y, Noh Y, Dudhia J. A new vertical diffusion package with an explicit treatment of entrainment processes. *Monthly Weather Review,* Vol. 134, No. 9, 2318–2341, 2006.

[17] Fairall C W, Bradley E F, Hare J E, Grachev A A, Edson J B. Bulk parameterization of air-sea fluxes: Updates and verification for the COARE algorithm. *JOURNAL OF CLIMATE*, Vol. 16, No. 4, pp 571-591, 2003.

[18] Chen F, Dudhia J. Coupling and advanced land surface-hydrology model with the Penn State-NCAR MM5 modeling system. Part I: Model implementation and sensitivity. *Monthly Weather Review,* Vol. 129, No. 4, pp 569–585, 2001.

[19] Kain J. The Kain‐Fritsch convective parameterization: An update. *Journal of Applied Meteorology*, Vol. 43, No. 1, pp 170–181, 2004.

[20] Chen S H, Sun W Y. A One-dimensional Time Dependent Cloud Model. *Journal of the Meteorological Society of Japan*, Vol. 80, No. 1, pp 99–118, 2002.

[21] Hong S Y, Lim J O J. The WRF single‐moment 6‐class microphysics scheme (WSM6). *Journal of the Korean Meteorological Society*, Vol. 42, pp 129–151, 2006.

[22] Morrison H, Thompson G, Tatarskii V. Impact of cloud microphysics on the development of trailing stratiform precipitation in a simulated squall line: Comparison of one‐ and two‐moment schemes. Monthly Weather Review, Vol. 137, No. 3, pp 991–1007, 2009.

[23] Thompson G, Field P, Rasmussen R, Hall W. Explicit forecasts of winter precipitation using an improved bulk microphysics scheme. Part II: Implementation of a new snow parameterization. *Monthly Weather Review*, Vol. 136, No. 12, pp 5095–5115, 2008.